Research Article GU J Sci 38(1): x-x (2025) DOI: 10.35378/gujs.1474009

Gazi University

Journal of Science

http://dergipark.gov.tr/gujs

Experimental Spectroscopic and Computational Studies on A New Synthesized Sulfisoxazole Derivative; Molecular Docking, Drug-likeness, ADME, Toxicity Predictions and Carbonic Anhydrase II Activity Investigations

Mustafa Tugfan BILKAN[1,*], Mehmet Fatih KARATAS[2], Cigdem BILKAN[3], Hamit ALYAR[1], Saliha ALYAR[2]

[1]*Tokat Gaziosmanpaşa University, Faculty of Medicine, 60230, Tokat, Türkiye*
[2]*Çankırı Karatekin University, Faculty of Science, 18100, Çankırı, Türkiye*
[3]*Tokat Gaziosmanpaşa University, Erbaa Vocational School of Health Services, 60500, Tokat, Türkiye*

Highlights

- A new sulfisoxazole derivative and its copper complex were synthesized.
- Structure analyses of the compounds were carried out using experimental and computational methods.
- CHNS, FT-IR, NMR, LC-MS, conductivity, magnetic susceptibility and TGA methods were used.
- Biological activity profiles of the compound were investigated in silico.
- Molecular docking studies were carried out to determine protein-ligand interactions.

Article Info

Received: 08 May 2024
Accepted: 10 Oct 2024

Keywords

Sulfisoxazole Derivatives, Quantum chemical calculations, Vibrational spectroscopy, Molecular docking, In silico predictions

Abstract

In this paper, 5-Dimethylamino-2-hydroxy-3-methoxy benzaldehyde sulfisoxazole (5DHMS) and Cu(5DHMS)$_2$ compounds have been synthesized. The molecular structure characterizations were performed using experimental and computational methods. In the experimental part of the study, CHNS, FT-IR, NMR, TGA, and LC-MS analysis techniques were used. Density Functional Theory (DFT) was selected for the calculation level in the theoretical part. Firstly, optimized structures were obtained from the predicted 3D structures. Vibrational modes were calculated using the optimized structures of the compounds. The vibrational modes of each compound were analyzed in detail using potential energy distribution (PED). Molecular electrostatic potential and HOMO-LUMO maps were drawn. Global chemical reactivity descriptors of compounds were determined. Moreover, the effects of solvent media on chemical reactivity descriptors were revealed in detail. Protein-ligand interactions with the target receptor carbonic anhydrase II enzyme were performed. In addition, some essential biological activity parameters such as drug-likeness, toxicity, and ADME predictions were examined in silico.

1. INTRODUCTION

Antibiotics are a group of drugs that are effective on bacteria and some types of parasites and are used to treat infections caused by them. Antibiotics, also called antibacterial or antimicrobial, can be found in many forms and structures, such as tablets, solutions, ointments, creams, lotions, etc. Nowadays, many antibiotic groups have gained a place in clinical treatment. Some of the most commonly used among these are sulfonamides. Sulfonamides, especially in treating bacterial infections, are one of the influential drug groups used systemically. This group of drugs is known as broad-spectrum antibiotics due to its bacterial growth inhibitory (bacteriostatic) effects. Especially towards the mid-1900s, research on new derivatives with fewer side effects and more effectiveness gained momentum. As a result of this type of research, a critical decrease in diseases caused by bacteria has been detected.

Sulfa drugs, also known as agents containing sulfonamide derivatives with antimicrobial effects, have been used for many years to treat many infections due to their low side effects, relatively low toxicity, and cheap

*Corresponding author, e-mail: mustafa.bilkan@gop.edu.tr

production costs [1]. For example, mafenide, a type of sulfa drug, is one of the drugs frequently used today in the form of mafenide acetate in burn treatment [2]. Similarly, sulfadiazine, another sulfa drug, is used for infections in the urinary tract [3], and sulfapyridine is one of the sulfa drugs used especially in treating skin and throat infections [4]. Although their use decreased after the 1940s when penicillin began to be used in the treatment of infections, and the bacterial resistance to sulfa drugs increased, after the 1970s, new mixtures of sulfa drugs produced with dihydrofolate reductase inhibitors such as trimethoprim, trimethylamine, and diaminopyrimidine began to be used frequently again. Another important medical application of sulfa drugs is their use as diuretics and antidiabetics. Especially after the 1950s, studies showing high diuretic activity of sulfonamides were published [5, 6]. In addition, in the late 1990s, Sildenafil Citrate, Amprenavir, and Celecoxib were introduced to the market as painkillers in treating rheumatism and meniscus [7]. It has been extensively researched after the 2000s that sulfonamides show anti-inflammatory, antiepileptic, antineoplastic, and antiretroviral effects and can be used for this purpose [8].

Their antibacterial, antifungal, anti-inflammatory, antiepileptic, antineoplastic, and antiretroviral effects cause the number of studies on sulfa drugs to increase rapidly. Mondal and Malakar have published a comprehensive review study on sulfonamide synthesis and its therapeutic applications [9]. They explained some critical details of the clinical and therapeutic applications of sulfonamides. In 2021, Wan et al. investigated the potential anticancer effects of sulfonamide derivatives. In the study, they summarized in detail the recent developments in sulfonamides as potential anti-cancer agents. [10]. In another study published recently, the structures, antibacterial properties, toxicities, and physicochemical parameters of sulfa drugs were determined [11]. The mechanism of action of sulfa drugs was also described in the study. Last year, Venkatesan et al. published a study on the molecular mechanism of antibiotic resistance of sulfa drugs [12]. An experimental and theoretical study was published by Dege et al. in 2022 on the structural, spectroscopic, biological, and physicochemical properties of sulfonamides [13]. We recently published studies on novel sulfonamide derivatives' production, characterization, and biological activity [14, 15].

In this study, we aimed to synthesize a new sulfisoxazole derivative and its copper complex to produce new types of drugs against increasing antibiotic resistance. The new potential drug and its metal complex were characterized by experimental CHNS, NMR, FT-IR, thermogravimetric (TGA), and liquid chromatography-mass spectrometry (LC-MS) analysis methods. Additionally, characterization was supported with theoretical methods. Molecular docking, absorption, distribution, metabolism, excretion (ADME), drug-likeness, and toxicity studies were also performed to obtain the pharmacological and biological properties of the molecules.

2. MATERIAL METHOD

2.1. Measurement and Analysis Systems

All of the chemical compounds used in the experimental parts of the study were provided by Merck Company. The chemicals supplied and used in experimental studies were not subjected to any purification process. FT-IR spectra of the compounds were recorded in the range of 4000-400 cm^{-1} by using FT-IR/Perkin-Elmer RX-1 Mattson-1000 Model spectrophotometer. The UV-visible spectra were recorded in the 200-800 cm^{-1} range with UNICAM-UV 2-100 equipment. CHNS analyses were done with a LECO-CHSNO–9320 elemental analysis device. The sample's carbon and proton NMR spectra were obtained with a 14.1 Tesla at 600 MHz frequency Agilent brand Premium Compact device. Magnetic susceptibility measurements were taken for the produced compounds using the Sherwood Scientific MKI model Gouy balance. The SRS Optimelt model, a melting point device, was used to determine the melting points of the complexes. Additionally, conductivity measurements of the compounds were carried out in methanol solution at 20 ºC with a Siemens WPA CM 35 conductivity meter. Waters 2695 Alliance Micromass ZQ instrument was used for recording LC-MS spectra. Finally, the complexes' TGA analyses were carried out using Du Pont Instrument 10951 device in a nitrogen atmosphere. The heating rate was ten ºC/min, and the temperature range was between 300-400 ºC.

2.2. The Synthesis of Compounds

0.15 g ($9.8x10^{-4}$ mol) 2-Hydroxy 4-(diethylamino)benzaldehyde dissolved in 10 mL ethanol and 0.263 g ($9.8x10^{-4}$ mol) sulfamethoxazole dissolved in 10 mL ethanol were mixed. The resulting mixture was heated and stirred for 30 minutes. The orange particles began to precipitate, and to complete the precipitation, they were refluxed at 60 ºC at 400 rpm for one day. The resulting product was stored in the freezer for one day. After crystallization from ethanol, it was filtered and washed with ether. The filtrate was dried in an oven at about 60 ºC and placed in a desiccator. M.P: 224–226 ºC, Yield: 82-84 %, M. W: 430.13 g/mol. The production scheme of 5DHMS is given in Figure 1.

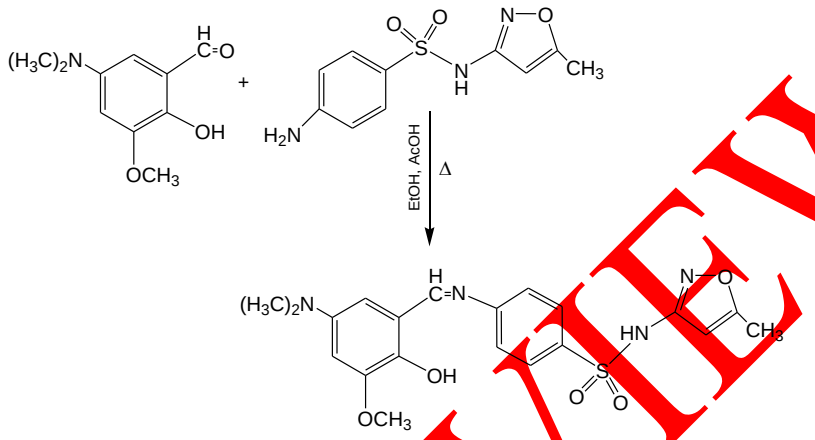

Figure 1. *The synthesis procedure scheme of 5DHMS*

In 30 mL of EtOH, 0.15 g ($3.7x10^{-4}$ mol) of 5DHMS dissolved was added to 0.015 g ($3.7x10^{-4}$ mol) of NaOH dissolved in 5 mL of EtOH. The mixture was stirred for about 15 minutes, and later, 0.055 g ($1.9x10^{-4}$ mol) $CuCl_2.2H_2O$ dissolved in 2 mL of pure water was added. The resulting mixture was mixed under the reflux mechanism for one day. The formed yellow precipitates were left in the deep freezer for two nights. The precipitates were filtered and washed with EtOH. Later, yield at about 150 °C dried in a vacuum desiccator. Molecular Weight: 936.24 g/mol, Yield: 83-85 %, M.P: 268-270 ºC. The production scheme of $Cu(5DHMS)_2$ is given in Figure 2. Additionally, the calculated and found elemental analysis results of the compounds are given in Table 1.

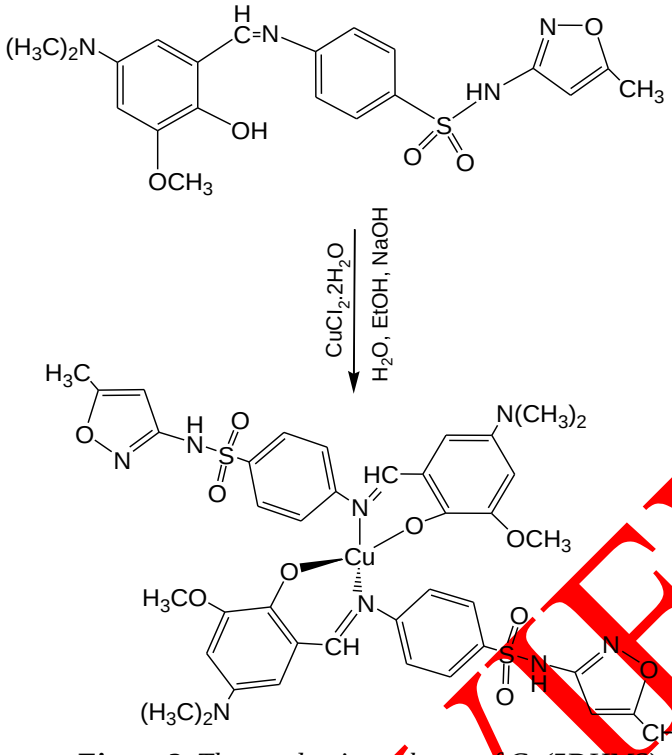

Figure 2. *The production scheme of Cu(5DHMS)$_2$*

Table 1. *Calculated and found elemental analysis results of the compounds (%)*

Compound	Calculated				Found			
	C	H	N	S	C	H	N	S
$C_{20}H_{22}N_4O_5S$	55.80	5.15	13.02	7.45	55.55	5.70	13.25	7.80
$C_{41}H_{45}CuN_8O_{10}S_2Cu$	52.53	4.84	11.95	6.84	52.55	4.10	11.75	6.80

As can be seen from the table, the calculated and experimental CHNS values are in good agreement with each other.

3. CALCULATION DETAILS

It is crucial to choose the right program and appropriate calculation levels in order to optimally determine the chemical, physical, spectroscopic, biological, and pharmacological properties of a molecular structure using computational methods. The first critical step in calculating the parameters of the molecule mentioned above is optimization. Density Functional Theory (DFT) is a theory whose reliability has been proven, especially in molecular structure calculations. The predicted structures of the molecules examined in this study were drawn in the Gausview program [16] and optimized with Gaussian09 [17]. Optimized structures were obtained at Becke's three-parameter hybrid exchange functional and the Lee-Yang-Parr (B3LYP)/6-311++G(d,p) and LanL2DZ levels. Based on the optimized structures, structural properties such as geometric parameters, thermochemical properties, atomic charges, vibrational frequencies, and HOMO-LUMO energies of the molecules were determined. The calculated vibrational modes were scaled by 0.9668 to eliminate deficiencies from the calculation level. Additionally, all vibrational modes were characterized using PED values using the VEDA4 program [18]. Global reactivity descriptors of the molecules were determined according to the procedures described by Parr [19]. The Molegro Virtual Docker MVD 2019.7.0 program was used to analyze intermolecular interactions between proteins and compounds [20]. Absorption, distribution, metabolism, excretion (ADME), toxicity, and drug-likeness estimates of each compound were obtained using the PreADMET [21] and Protox-II [22] suite.

4. RESULTS AND DISCUSSION

4.1. Vibrational Modes and Assignments

The vibration movements between the atoms that make up a molecule can provide useful information in determining the molecular structure. Molecular vibrational spectroscopy supports acquiring these atomic vibrational movements by experimental and computational methods, thus characterizing the structure. In the presence of n number of atoms forming a nonlinear molecule, apart from rotation around three axes and translation in three axes, it creates 3n-6 degrees of freedom constitute vibrational motion.

It is seen from Figure 2 that a covalently bonded $Cu(5DHMS)_2$ structure was formed between the Cu atom and two 5DHMS molecules. Accordingly, 5DHMS has 52 atoms and thus 150 fundamental vibrational modes, and the $Cu(5DHMS)_2$ complex has 103 atoms and 303 fundamental vibrational modes. Some important selected vibrational modes are given in Table 2. The recorded FT-IR spectra of the compounds are presented in Figure 3.

Table 2. *Experimental and calculated selected vibrational modes and PED values of 5DHMS and* $Cu(DHMS)_2$

Mode	$Cu(5DHMS)_2$				Mode	5DHMS			
	Calc.	I_{IR}	Exp.	PED (%)		Calc.	I_{IR}	Exp.	PED (%)
87	429	6.42	425 w	$\delta_{OCC}(20)$	48	609	11.84	613 m	$\tau_{NCCC}(36)$
90	470	18.14	483 w	$\tau_{ONOS}(24)$	52	643	28.89	645 w	$\tau_{ONOS}(13)+\delta_{OCC}(10)+V_{SC}(10)$
106	598	1.11	605 vs	$\tau_{NNCC}(21)$	53	686	1.97	696 w	$\tau_{CONC}(38)+\tau_{CCON}(21)+\tau_{ONCN}(12)$
111	624	0.58	635 s	$\tau_{NNCC}(22)$	55	726	1.99	711 m	$\delta_{CCC}(12)$
115	664	2.56	678 s	$\tau_{NNCC}(14)$	56	736	1.92	740 m	$\tau_{OCCC}(55)$
119	715	2.63	701 s	$\tau_{CCCC}(38)$	59	781	10.00	784 w	$\tau_{HOCC}(93)$
125	766	4.33	763 m	$\tau_{OCCC}(24)$	64	829	6.38	839 s	$\tau_{HCNC}(25)+V_{SN}(19)$
129	795	11.98	817 s	$\tau_{HCCN}(28)+\tau_{HCCC}(24)$	67	867	5.23	862 m	$V_{NC}(27)+\delta_{HCC}(11)$
140	864	10.74	842 s	$\tau_{HCCC}(74)$	73	970	2.42	976 m	$\tau_{HCNC}(67)$
145	891	1.53	905 m	$V_{OC}(36)+V_{SO}(22)$	76	992	1.78	997 w	$\delta_{CCC}(69)$
157	988	2.78	987 m	$\tau_{HCCC}(34)$	77	1006	1.77	1012 w	$V_{OC}(33)+\delta_{CCO}(33)+V_{NC}(10)$
164	1003	1.02	1013 m	$\tau_{HCCC}(56)$	83	1089	58.87	1094 m	$V_{SO}(54)+V_{SN}(10)$
166	1045	5.68	1032 m	$V_{CC}(59)$	91	1191	26.93	1197 m	$V_{NC}(22)+\delta_{HCC}(11)+V_{CC}(11)$
172	1060	5.15	1092 vs	$\delta_{HCC}(28)+V_{SO}(24)$	96	1256	9.38	1253 m	$V_{OC}(34)+\delta_{HCC}(12)$
184	1145	9.62	1142 vs	$\tau_{HCOC}(33)$	100	1289	17.32	1280 w	$V_{CC}(37)$
191	1187	4.20	1199 s	$V_{OC}(22)$	101	1331	46.98	1343 s	$\delta_{HCN}(30)+V_{CC}(13)$
198	1252	7.36	1250 s	$V_{NC}(45)$	103	1362	14.66	1376 w	$\delta_{HCN}(27)+V_{CC}(10)$
201	1272	11.22	1288 s	$\delta_{HNC}(58)+V_{NC}(15)$	108	1422	15.40	1419 s	$V_{NC}(21)+\delta_{HCH}(21)+\delta_{ONC}(18)$
210	1372	19.76	1370 s	$V_{CC}(62)$	116	1445	16.73	1449 m	$\delta_{HCH}(28)+\delta_{ONC}(10)$
226	1435	16.15	1442 s	$\delta_{HCH}(30)$	121	1478	16.29	1460 m	$\delta_{HCH}(37)$
248	1503	30.53	1483 s	$\delta_{HCH}(24)$	124	1556	100.00	1573 m	$V_{NC}(13)+V_{CC}(13)$
252	1547	24.38	1533 s	$V_{NC}(26)+\delta_{HCC}(11)$	125	1578	4.88	1589 s	$V_{CC}(31)+\delta_{HOC}(11)$
260	1604	100	1592 vs	$V_{NC}(29)+V_{CC}(22)$	127	1593	29.20	1615 m	$V_{CC}(26)+V_{NC}(20)$
282	3060	10.84	2970 vw	$V_{CH}(92)$	128	1609	18.47	1645 w	$V_{NC}(26)+V_{CC}(10)$
298	3141	1.59	3243 w	$V_{CH}(99)$	139	3019	7.46	2836 vw	$V_{CH}(94)$
301	3220	0.42	3280 w	$V_{CH}(99)$	148	3168	89.89	2934 vw	$V_{OH}(99)$
303	3494	4.05	3391 w	$V_{NH}(100)$	150	3432	7.45	3192 vw	$V_{NH}(100)$

* Selections of vibrational modes were made from among the most intense. V: stretching, δ: bending, τ: torsional, **vs: very strong, s: strong, m: medium, w: weak, vw: very weak

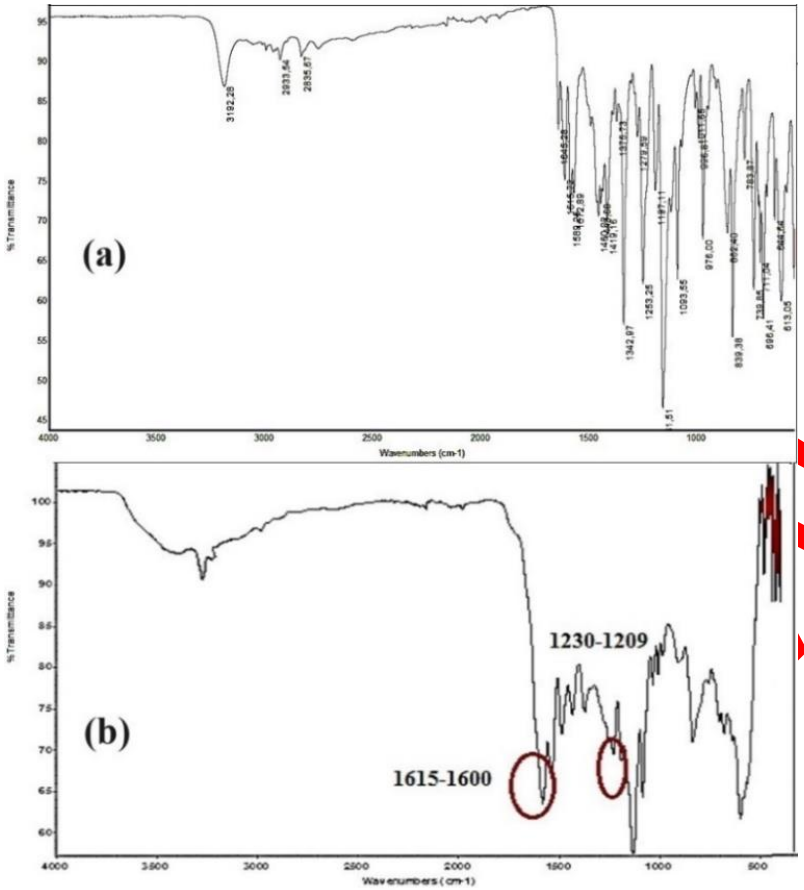

Figure 3. *Experimental FT-IR spectra of (a) 5DHMS and (b) Cu(5DHMS)$_2$*

The strong band observed at 3192 cm^{-1} in the FT-IR spectrum is the secondary amine (NH) stretching mode. This mode was calculated at 3492 cm^{-1}. The reason for the difference between experimental and calculated values is that the experimental records are recorded under the presence of too many intra- and intermolecular interactions. In contrast, the calculated mode is obtained for a single molecule in the gas phase. The ν(N-C) vibrational modes were observed at 1645(w), 1573(m) and 1419(s), 1197(m) and 862(m) cm^{-1} for 5DHMS in accordance with the literature [23]. The calculated N-C stretching modes were obtained at 1609, 1556, 1422, 1191 and 867 cm^{-1}. For 5DHMS, the medium intense band observed at 1615 cm^{-1} was assigned as ν(C=N) imine vibration. It shifted to 1592 cm^{-1} for Cu(5DHMS)$_2$ as strong. This vibration wavenumber decreases to low values due to the formation of the metal complex. This shows that the unshared electron pairs of the imine nitrogen of 5DHMS are shared with the copper atom due to covalent bonding. This leads to a weakening in the C=N bond. The detected stretching mode at 1253 cm^{-1} belongs to the ligands ν(C-O) vibration motion. It shifted to a low wave number and was observed at 1199 cm^{-1} as moderate intensity in the complex formation. This shift confirms that the phenolic oxygen is coordinated to the metal cation. For the resulting complex, the donor nitrogen atom in the NH group around the sulfamethoxazole ring did not bond with the metal due to steric effects. According to the table, there is no significant change in both the experimental and calculated values of SO_2 vibrations after complex formation, which is another important indicator that the coordination to the metal atom is not made from these groups. The vibrational modes observed in the experimental spectra of compounds in the 2800-3200 cm^{-1} region belong to aromatic C-H stretching [24]. These modes were calculated at the same region. The small differences between the calculated values of the vibrations in this region and the experimental ones are mostly due to intermolecular and sometimes intramolecular interactions. While experimental spectra are recorded in phases where many molecules interact, theoretical calculations are performed for a single molecule without intermolecular interaction. For this reason, differences may arise between the two.

4.2. ^{13}C-^{1}H NMR Chemical Shift Analyses

^{1}H and ^{13}C-NMR chemical shifts of the ligand were investigated via experimental results recorded in DMSO-d6. Both experimental spectra are depicted in Figure 4. Moreover, the chemical shift values are given in Table 3.

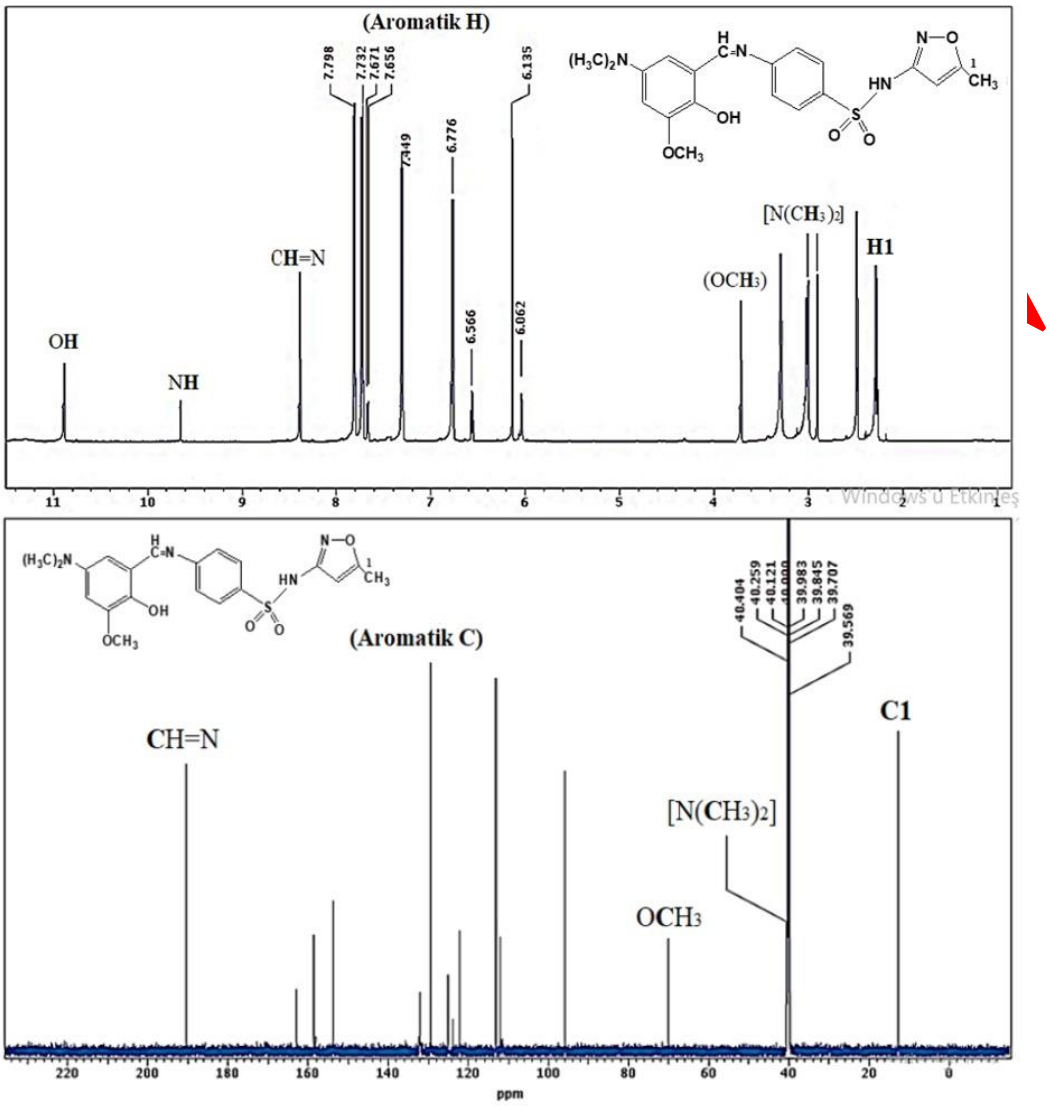

Figure 4. *^{1}H-^{13}C NMR spectra of 5DHMS*

Table 3. *Experimental ^{1}H and ^{13}C NMR chemical shift values δ(ppm) of 5DHMS*

Assignments	δ(Exp)	Assignments	δ(Exp)
C1(CH_3)	16.49	**NCH_3**	2.99
C4 (CH_3)	-	**OCH_3**	3.76
(CH=N)	191.60	**Aromatic H**	6.07-7.80
$(NCH_3)_2$	40.52	**CH=N**	8.38
OCH_3	69.80	**NH**	9.68
Aromatic C	96.00-162.02	**OH**	10.76
NCH_3	3.09	**H1**	2.30

5DHMS contains fifteen aromatic, four methyl, and one imine carbons. Aromatic carbons give signals between 120-150 ppm [25, 26]. In the ^{13}C-NMR spectrum of the ligand, aromatic carbon signals were observed in the specified region, consistent with the literature. While $N(CH_3)_2$ vibrations concentrated

around 40 ppm, C_1 and OCH_3 carbon signals were recorded as 16.49 ppm and 69.80 ppm. CH=N (imine) carbon gave a signal at 191.60 ppm.

In the proton NMR spectrum of 5DHMS, H_1, OCH_3, and $N(CH_3)_2$ protons are marked at 2.30, 2.99, 3.09, and 3.76 ppm, respectively. The observed signal for CH=N (imine) proton is at 8.38 ppm. The experimental values of the NH proton and phenolic OH proton are marked at 9.68 and 10.76 ppm as weak intensity. Additionally, the peaks of aromatic protons (Ar-H) of 5DHMS were observed between 6.07-7.80 ppm.

4.3. Global Chemical Reactivity Descriptors and HOMO-LUMO Analysis

In computational chemistry, the determination of Highest Occupied Molecular Orbital (HOMO) and Lowest Unoccupied Molecular Orbital (LUMO) energies is one of the most critical phenomes. These energies are used to calculate some crucial parameters of molecules, such as polarity, hardness, softness, basicity, acidity, and excitability, also known as global reactivity descriptors. Moreover, electronic transitions and charge transfer can be obtained based on HOMO-LUMO values [27]. Besides, the HOMO-LUMO maps of compounds provide valuable data related to the bonding and anti-bonding character. For 5DHMS and $Cu(5DHMS)_2$ compounds, HOMO-LUMO maps are presented in Figure 5.

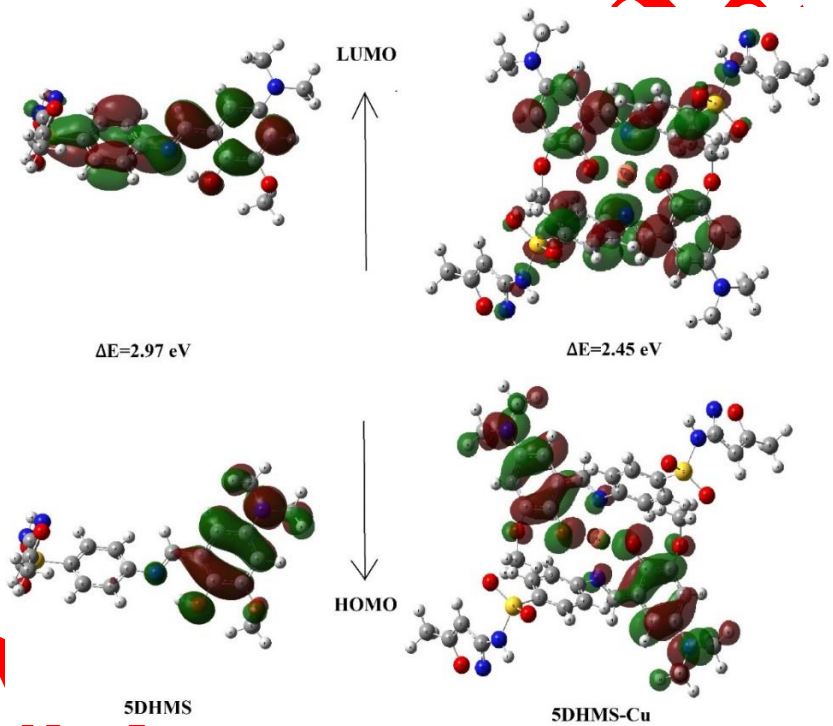

Figure 5. *The contour maps of HOMO-LUMO levels for 5DHMS and $Cu(5DHMS)_2$ compounds*

In the vacuum, EtOH, DMSO, and water media, calculated chemical potential (μ), electron affinity (A), ionization potential (I), global hardness (η), and electrophilicity (ω) values are presented together with HOMO-LUMO energies in Table 4.

Table 4. *The calculated reactivity data for the compounds*

Parameters	5DHMS				$Cu(5DHMS)_2$			
	Vacuum	EtOH	DMSO	Water	Vacuum	EtOH	DMSO	Water
E_{LUMO}	2.46	2.45	2.45	2.45	2.63	2.65	2.65	2.65
E_{HOMO}	5.43	5.37	5.38	5.38	5.08	4.99	4.99	4.99
$\Delta E_{LUMO-HOMO}$	1.48	1.46	1.46	1.46	1.23	1.17	1.17	1.17
Electron affinity (A)	-3.95	-3.91	-3.91	-3.91	-3.86	-3.82	-3.82	-3.82
Ionization potential (I)	5.25	5.23	5.23	5.23	6.07	6.22	6.23	6.24

Global hardness (η)	2.46	2.45	2.45	2.45	2.63	2.65	2.65	2.65
Chemical potential (μ)	5.43	5.37	5.38	5.38	5.08	4.99	4.99	4.99
Electrophilicity (ω)	1.48	1.46	1.46	1.46	1.23	1.17	1.17	1.17

As seen from Table 4, the calculated HOMO-LUMO energy gap, an essential indicator of molecular stability, has been severely affected by the changing solvent environment. Additionally, the HOMO-LUMO gap decreased significantly with copper complex formation.

4.4. Molecular Electrostatic Potential (MEP) Analysis

Molecular electrostatic potential (MEP) mapping is a widely used analysis to determine a compound's most reactive sites and positions. This feature is frequently used to examine the intermolecular hydrogen bonding of compounds [28].

Standard MEP maps contain blue, green, yellow, and red regions. Generally, unless otherwise stated, the red regions are parts of compounds with the most negative charges and potential. In that region, negatively charged atoms, such as nitrogen or oxygen atoms, are located. Blue color regions are more positive parts of a molecule. Yellow and green regions are relatively neutral or near-neutral parts of the molecule. The regions where intermolecular interactions occur most strongly are the parts where red is most intense.

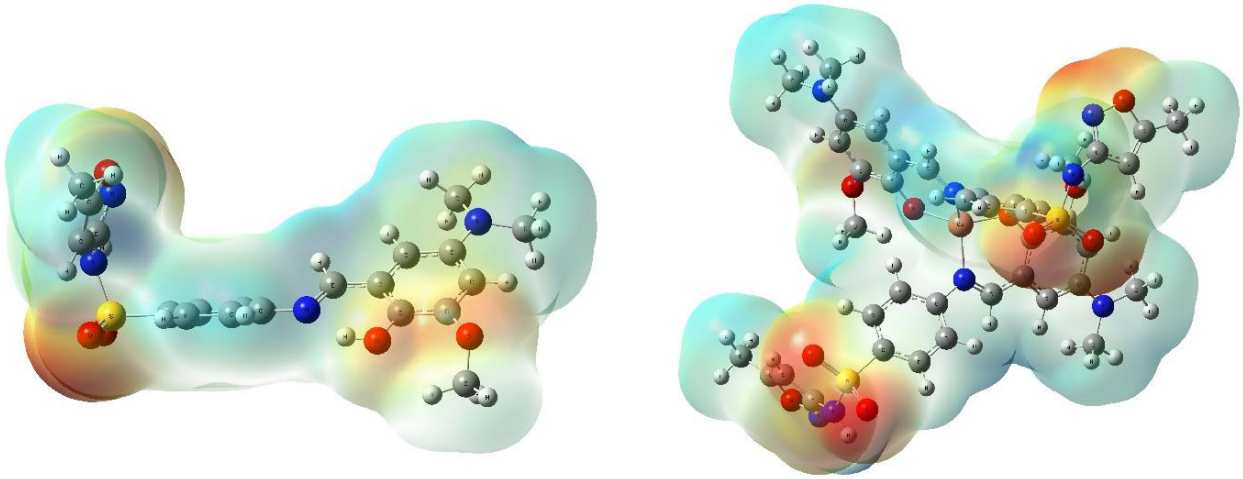

Figure 6. *The molecular electrostatic potential maps of 5DHMS and Cu(5DHMS)$_2$ compounds*

When Figure 6 is investigated in detail, it is seen that the MEP maps of both synthesized compounds involve red parts in regions of C-O and S=O group locations. These parts of the compounds serve as hydrogen acceptors in the intermolecular hydrogen bonds they establish. All hydrogen atom sites for 5DHMS and the copper compound appear blue, but especially the hydrogen atoms attached to the hydroxyl and amine groups contain more positive charges than the others. The yellow and green regions present in small amounts are the neutral regions of the molecules.

4.5. LC-MS, TGA, Magnetic Susceptibility and Conductivity Analysis

The use of new analysis techniques in studies on drug development has accelerated the developments in this field. The combination of high-performance liquid chromatography and mass spectrometry (LC/MS) has become one of the essential qualitative and quantitative structure analysis techniques in the last decade, especially in drug development studies [29].

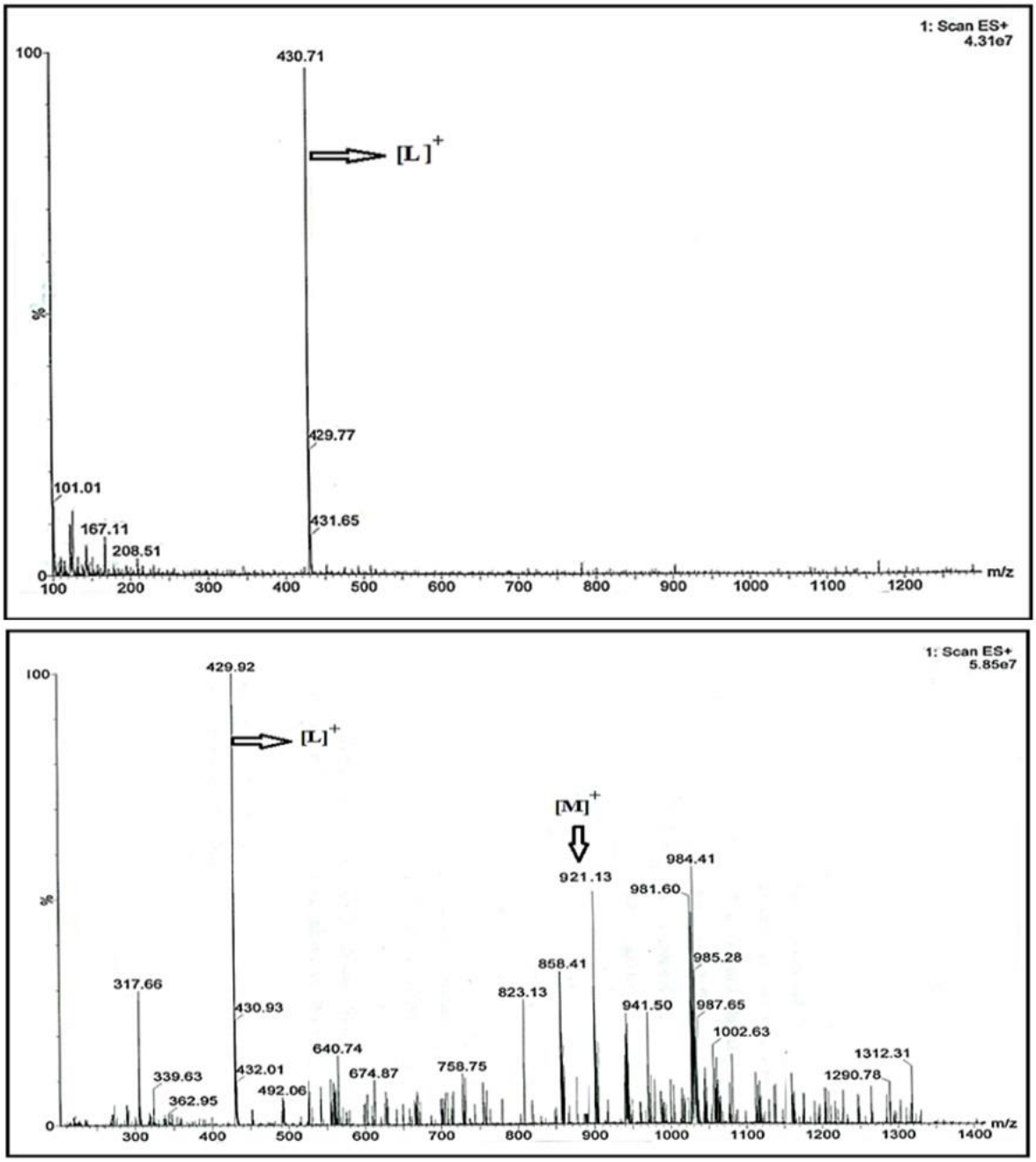

Figure 7. *LC-MS spectra of 5DHMS and Cu(5DHMS)$_2$ compounds*

The experimental LC-MS spectra of 5DHMS and Cu(5DHMS)$_2$ are presented in Figure 7. The figure shows that the molecular ion peaks for both compounds are observed at $[L]^+$= 430.71 and $[M]^+$= 921.13 for the ligand and copper complex.

TGA is another important analysis method in chemical studies. In TGA measurements, the loss in mass of the substance with changing temperature is analyzed depending on time.

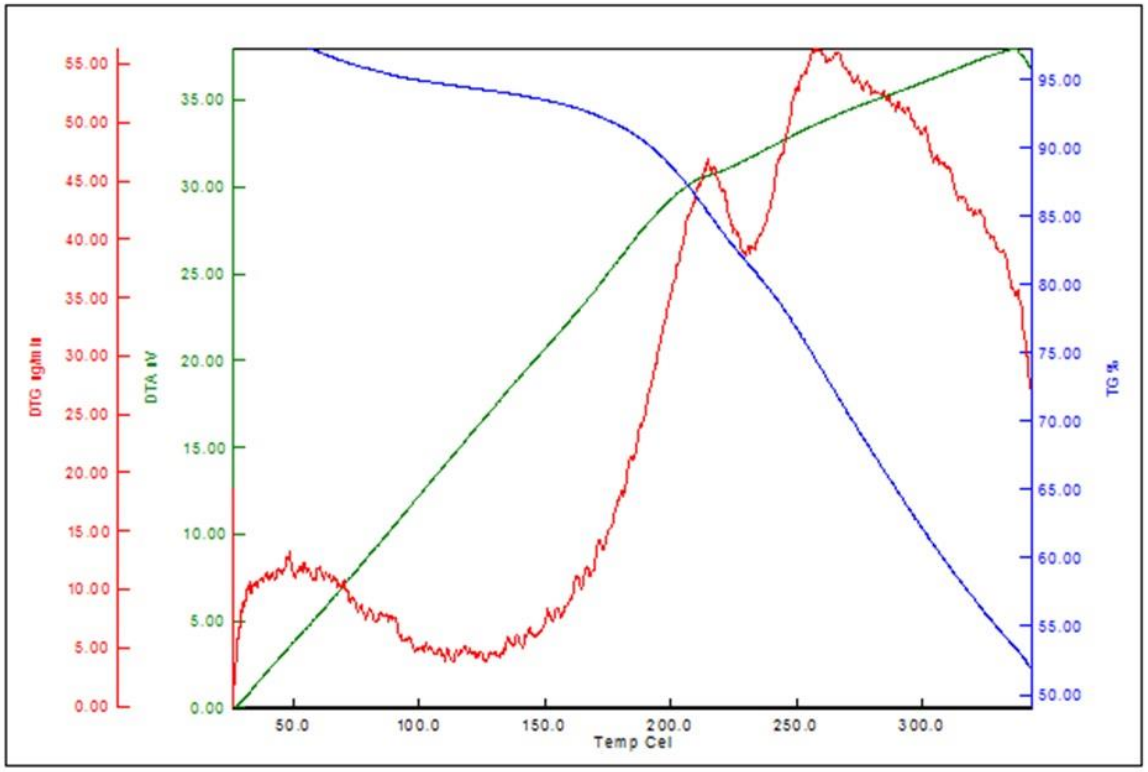

Figure 8. *TGA curve of Cu(5DHMS)$_2$*

Figure 8 shows the TGA curve of Cu(5DHMS)$_2$ compounds. The fact that there is no significant mass loss in the compound mass until the temperature reaches 220 ºC reveals no crystal water in the structure of the complex.

Magnetic susceptibility measurements were also made for the Cu(5DHMS)$_2$ compound. Magnetic susceptibility is an indicator of the extent to which the sample will be magnetized in a magnetic field. Magnetic susceptibility measurements made for the copper compound in this study showed that the produced complex has a paramagnetic character and determined effective magnetic moment (μ_{eff}) of the compound is 2.22 BM.

In molar conductivity (ΛM) measurements of Cu(5DHMS)$_2$, used DMSO solution was prepared as $1x10^{-3}$ M. As a result of the measurement, the ΛM value is obtained to be 16.5 $ohm^{-1}.cm^2$/mol. This shows Cu(5DHMS)$_2$ is a non-electrolyte material.

4.6. Carbonic Anhydrase II (hCAII) Inhibition Results

The Carbonic Anhydrase Enzyme (CAE) catalyzes the conversion of carbon dioxide to proton and bicarbonate, a relatively slow biochemical process. Its active parts contain zinc; in this respect, it is a metalloenzyme [30]. CAEs have great medical importance and are also critical potential targets in using some crucial drugs [31]. They are a research area for diseases such as cancer and Alzheimer's [32]. In this paper, the inhibition effects of 5DHMS and Cu(5DHMS)$_2$ were investigated on CAE. The p-nitrophenyl acetate solution used as substrate in the experimental study was prepared daily. 3 mM stock solution of the substrate was prepared and adjusted to be 0.3, 0.6, 1.0, and 3.0 mM concentrations. Substrate and buffered enzyme solution (0.05 M Tris-SO4 pH= 7.4) were placed in quartz cuvettes at 25 ˚C and the absorbance value was read against the blank at 348 nm for 3 minutes. In the investigation of the inhibitory effects of alkyl sulfonic acid hydrazide inhibitors on CA-II enzyme, IC50 values (inhibitor concentration causing 50% inhibition) were calculated. Acetazolamide (ACZ) was used to compare inhibitory activity. It is a widely used carbonic anhydrase inhibitor that prevents carbonic acid's breakdown. A graphical image showing the comparison of the inhibitory effects of ACZ, 5DHMS, and Cu(5DHMS)$_2$ is given in Figure 9.

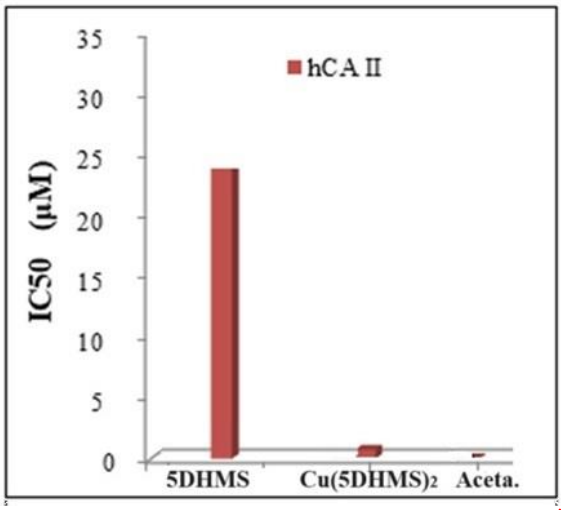

Figure 9. *Comparison of inhibitory effects of acetazolamide and compounds*

The figure shows IC50 (inhibitor concentration reduces enzyme activity by half) values for 5DHMS, $Cu(5DHMS)_2$, and the reference molecule ACZ. The obtained IC50 values were 23 µM for 5DHMS, 0.73 µM for $Cu(5DHMS)_2$, and 0.017 µM (17 nm) for the reference molecule ACZ. The results revealed that both compounds showed higher inhibitory effects compared to ACZ. However, 5DHMS showed a much higher inhibitory effect than the copper complex.

4.7. ADME, Drug-likeness and Toxicity Parameters of the Compounds

Determining the ADME processes of a molecule with pharmacological activity can provide important information about the molecule's effectiveness before clinical research and use. ADME defines a series of pharmacokinetic stages that begin with the distribution of drugs into the bloodstream after being taken into the living body and their excretion from the body through the liver and, ultimately, the renal system. Since experimental investigations of bioactivity are both high-cost and time-consuming processes, in silico examinations can provide beneficial preliminary information [33]. In addition, the entire journey of drugs in metabolism occurs in the solvent (water) environment. Therefore, ADME and solvent effects are also significantly related to each other. Therefore, this study aimed to determine ADME values after examining the solvent effects on the molecules produced. ADME parameters of both compounds were obtained with the PreADMET website; the results are tabulated in Table 5.

Table 5. *In silico predicted ADME values of 5DHMS and $Cu(5DHMS)_2$*

ID	5DHMS	$Cu(5DHMS)_2$
BBB	0.011	0.180
Caco2	11.99	23.12
HIA	95.12	90.34
MDCK	0.12	0.05
Plasma Protein Binding	89.29	100.00
Pure water solubility (mg/L)	174.81	1037.37

BBB refers to the penetration of a molecule into the blood-brain barrier. The limit value for BBB is around 2.00. Molecules with values of 2.00 and above are well absorbed by the CNS [34]. In this study, it was found that BBB=0.011 for 5DHMS and BBB = 0.180 for the copper complex. These results indicate the compounds are not well absorbed by the CNS. Caco2 expresses the permeability of the epithelial barrier of human colorectal carcinoma cells [35]. In silico Caco2 predictions are a model in which this permeability is determined and is another critical ADME parameter. The predicted Caco2 values are 11.99 nm/sec and 23.12 nm/sec for 5DHMS and $Cu(5DHMS)_2$, respectively. If P_{Caco2} is less than 4 nm/sec, it means low permeability; between 4 nm/sec and 70 nm/sec, it means medium permeability; and if it is greater than 70 nm/sec, it means high permeability [36]. This shows that both compounds have medium permeability. HIA

predicts human intestinal absorption of drugs. It can provide critical information in determining whether a molecule is a potential drug candidate. HIA shows what percentage of orally taken drugs can be absorbed from the gastrointestinal tract. HIA values for the compounds in this study were obtained as 95.12% and 90.34%. Both molecules show excellent absorption since values between 70% and 100% mean high gastrointestinal absorption. The Madin-Darby Canine Kidney (MDCK) cell line is widely used in biological studies as an epithelial cell model.

The MCDK permeabilities of 5DHMS and $Cu(5DHMS)_2$ were obtained as 0.12 and 0.05 nm/sec, respectively. One of the critical parameters that should be known for a potential drug candidate is plasma protein binding (PPB). After a drug is absorbed, it is expected to pass into the bloodstream and thus show its mechanism of action by circulating throughout the body. For this reason, it is important for drugs to bind with plasma proteins in the blood. The percentage of binding to plasma proteins is one factor that directly affects drug effectiveness. The PPB values calculated in this study are 89.29% and 100%. This suggests the circulatory properties of these potential drugs are high.

Some conditions provided by a newly synthesized molecule can provide useful information about its potential to be used as a drug. For this purpose, there are rules defined by Lipinski regarding the structural properties of molecules and called Lipinski's five rules [37]. Molecules that meet these conditions can be investigated as potential drug candidates. The first of these conditions is that the number of hydrogen bond donors of the molecule under investigation is less than 5, the second is that the weight of the molecule is less than 500 Dalton, the third is that the logP value is less than 5, and finally, the number of hydrogen bond acceptors is less than 10. Both produced molecules comply with Lipinski's rule of 5.

In a very general definition, toxicity is the degree to which a substance causes harm to a biological organism. Toxicity can affect a living thing, but it can also affect an organ or a single cell (or even a bacterium). With a philosophical discourse, all substances have a minimal non-toxic dose, while an overdose of all substances is toxic. So toxicity is completely dose-dependent. In this case, toxicity must be kept to a minimum when using a drug or a drug-candidate molecule in living systems. Especially hepatotoxicity and nephrotoxicity are the most critical negativities of drugs on the body. In silico toxicity parameters obtained in this study are shown in Table 6 for both compounds.

Table 6. *The predicted toxicity values of the compounds*

ID	**5DHMS**		**$Cu(5DHMS)_2$**	
Predicted LD_{50} (mg/kg)	4000	-	470	-
Predicted Toxicity Class	5	May be harmful if swallowed	4	harmful if swallowed
	Probability	**Prediction**	**Probability**	**Prediction**
Hepatotoxicity	0.58	Active	0.50	Active
Immunotoxicity	0.93	Active	0.98	Active
Cytotoxicity	0.84	Inactive	0.61	Inactive
Carcinogenicity	0.50	Inactive	0.51	Inactive
Mutagenicity	0.63	Inactive	0.63	Inactive

The most critical parameter to be determined in toxicity analyses is LD50 (Lethal dose 50%). LD50 is defined in toxicology as the dose value that kills 50% of the total population [38]. The higher the LD50 value of a substance, the lower the toxicity of that substance [39]. It can be seen from Table 6 that the LD50 value (mass of toxic substance per unit mass of the living thing) obtained for 5DHMS is 4000 mg/kg, while it is 470 mg/kg for $Cu(5DHMS)_2$. There is a significant difference between the two calculated values. The critical difference between these two LD50 values is due to the high toxicity of copper compounds [40]. However, the LD50 of 5DHMS is very close to that of the widely used anti-analgesic and antipyretic drug paracetamol (estimated to be approximately 340 mg/kg by the same *in silico* method). Studies in the literature reported that the experimental LD50 value of paracetamol was around 200 mg/kg [41]. This result reveals that in silico analyses closely correlate with experimental results. The toxicity class for 5DHMS

was also determined as 5, while for copper complex, it was estimated at 4. However, since both molecules have immunotoxic and hepatotoxic activity, it is recommended to consider LD50 values in pharmacological studies of these molecules.

4.8. Molecular Docking

New drug research is among the most important scientific issues of the past 10 years. Computer-aided studies, especially in the design phase, are becoming more and more prominent in the literature every day. Molecular docking allows examining especially ligand-protein interactions with the help of computers and thus determining how and to what extent the ligand binds to the protein. Carbonic anhydrase II enzyme was chosen as the target receptor in the molecular docking studies in this paper (PDB code: 2Q38; Resolution 1.95 Å). In silico ligand-protein examinations were carried out using the Molegro Virtual Docker MVD 2019.7.0 program and the results are given in Table 7.

Table 7. *Sulfonamide compounds-CA II Enzyme Interaction Docking Results*

Parameters	**5DHMS**	**Cu(5DHMS)$_2$**
MolDock Score	-129.093	-141.652
Rerank Score	-55.750	-74.206
Hydrogen Bonding energy (kcal/mol)	-5.57	-5.52
Steric Hindrance Energy	-108.709	-120.631
Electrostatic Interaction Energy	-1.673	1.284
Total Energy	-102.058	-105.236
Hydrogen Bond length with N atom on isoxazole ring of Asn61 (Å)	3.15	-
Hydrogen Bond length with N atom on SO_2 group of Asn61 (Å)	2.01	-
Hydrogen Bond length with N atom on isoxazole ring of Lys159 (Å)	-	2.47
Hydrogen Bond length with O atom on isoxazole ring of Lys159 (Å)	-	2.39

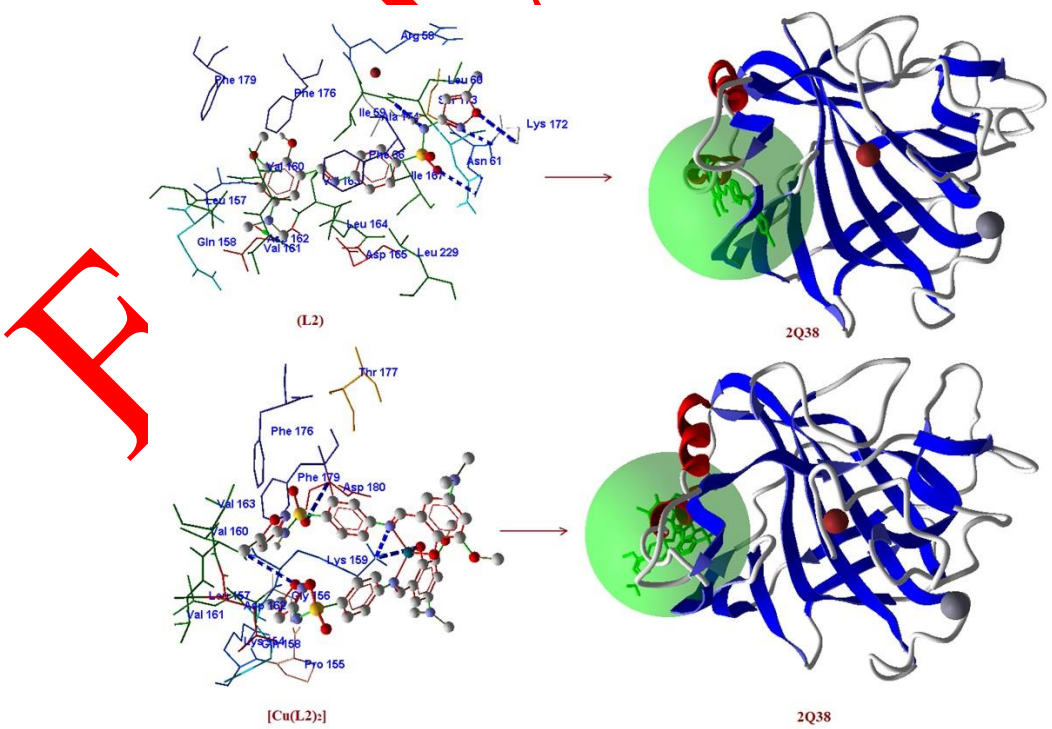

Figure 10. *Interactions of hCAII-5DHMS (top) and hCAII-Cu(5DHMS)$_2$ (bottom) compounds with the active sites of the protein (PDB:2Q38)*

As seen from the values in Table 7, the $Cu(5DHMS)_2$ compound is bound to the protein more strongly. Interactions between hCAII-5DHMS and hCAII-$Cu(5DHMS)_2$ compounds can be seen in Figure 10. In the figure, green dots represent active sites and thick dashed blue lines, hydrogen bonding, steric interactions, and unbound amino acids. It can be seen from Figure 10 that four hydrogen bonds were established between 2Q38 and the copper complex. The first of these bonds is the bond established between the N-H proton and the sulfonyl oxygen of the Asp180 amino acid of the protein and its length is 2.875 Å. The second hydrogen bond was established between the N atom in the isoxazole ring, and one of the NH3 protons of Lys 159 amino acid, and its value was obtained as 2.226 Å. The third h-bond interaction is established between the nitrogen bonded to the copper atom and another NH3 proton of Lys 159 and its size is 3.099 Å. The last hydrogen bond was established between the NH proton of Lys159 and the metal-bound oxygen atom of the copper complex (3.099 Å).

5. CONCLUSION

In this study, sulfamethoxazole-based ligand and its copper complex were synthesized for the first time. The structures of the synthesized molecule and the copper compound were characterized by experimental CHNS analysis and spectroscopic methods. Optimized geometries of the compounds were obtained by using the DFT method. Chemical reactivity describers, MEP, and HOMO-LUMO maps were elucidated. The in silico toxicity, drug-likeness, and ADME predictions of the ligand and the copper complex were also made. The magnetic susceptibility measurement and enzyme inhibition investigations were done. The results of the study can be summarized as follows:

- CHNS analysis results showed that two 5DHMS molecules were coordinated with a copper atom.
- For 5DHMS, the band observed at 1615 cm^{-1} ν(C=N) imine vibration shifted to 1592 cm^{-1} for $Cu(5DHMS)_2$ as strong. This shift is attributed to the formation of the metal complex. The unshared electron pairs of the imine nitrogen of 5DHMS are shared with the copper atom due to covalent bonding.
- The chemical reactivity descriptors were calculated in solvent media, and it is seen from the results that the changing solvent environment had significant effects on the calculated parameters.
- Magnetic susceptibility measurements on the copper complex reveal that the compound shows paramagnetic properties.
- Carbonic Anhydrase Enzyme inhibition of the $Cu(5DHMS)_2$ complex was found to be 0.73 µM, and that of the 5DHMS compound was 23 µM. This result showed the effect of $Cu(5DHMS)_2$ complex on enzyme inhibition was high.
- As a result of molecular docking studies, the energy of each binding state was calculated to determine the nature and size of the compounds' binding to the enzyme's active sites. It was observed that there were strong bonds between the enzyme and the copper complex.

CONFLICTS OF INTEREST

No conflict of interest was declared by the authors.

REFERENCES

[1] Parasca, O. M., Gheaţă, F., Pânzariu, A., Geangalău, I., Profire, L. "Importance of sulfonamide moiety in current and future therapy", Revista medico-chirurgicala a Societatii De Medici Si Naturalisti, April-June, 117: 558-564, (2013).

[2] Dai, T., Huang, Y. Y., Sharma, S. K., Hashmi, J. T., Kurup, D. B., Hamblin, M. R., "Topical antimicrobials for burn wound infections", Recent Patents on Anti-Infective Drug Discovery, 5: 124-51, (2010).

[3] Blondeau, J. M., and Fitch, S. D. "In vitro killing of canine urinary tract infection pathogens by ampicillin, cephalexin, marbofloxacin, pradofloxacin, and trimethoprim/sulfamethoxazole", Microorganisms, 9(11): 2279, (2021).

[4] Mushtaq, S., Sarkar, R., "Sulfasalazine in dermatology: A lesser explored drug with broad therapeutic potential", International Journal of Women's Dermatology, 13: 191-198, (2020).

[5] Edgar, Selvaag., "In Vitro Phototoxicity Due to Sulfonamide-Derived Oral Antidiabetic and Diuretic Drugs", Journal of Toxicology: Cutaneous and Ocular Toxicology, 16: 77-84, (1997).

[6] Renzi, A. A., Chart, J. J., Gaunt, R. R., "Sulfonamide compounds with high diuretic activity", Toxicology and Applied Pharmacology, 1(4): 406-416, (1959).

[7] Tang, C., Dong, X., He, W., Cheng, S., Chen, Y., Huang, Y., Yin, B., Sheng, Y., Zhou, J., Wu, X., Zeng, F., Li, Z., Liang, F., "Cerebral mechanism of celecoxib for treating knee pain: study protocol for a randomized controlled parallel trial", Trials, 20: 58, (2019).

[8] Petkar, P. A., Jagtap, J. R., "A Review on Antimicrobial Potential of Sulfonamide Scaffold", International Journal of Pharmaceutical Sciences Review and Research, 2: 2535-2547, (2020).

[9] Mondal, S., Malakar, S., "Synthesis of sulfonamide and their synthetic and therapeutic applications: Recent advances", Tetrahedron, 76(48): 131662, (2020).

[10] Wan, Y., Fang, G., Chen, H., Deng, X., Tang, Z., "Sulfonamide derivatives as potential anti-cancer agents and their SARs elucidation", European Journal of Medicinal Chemistry, 226: 113837, (2021).

[11] Ovung, A., Bhattacharyya, J., "Sulfonamide drugs: Structure, antibacterial property, toxicity, and biophysical interactions", Biophysical Reviews, 13(2): 259-272, (2021).

[12] Venkatesan, M., Fruci, M., Verellen, L. A., Skarina, T., Mesa, N., Flick, R., Savchenko, A., "Molecular mechanism of plasmid-borne resistance to sulfonamide antibiotics", Nature Communications, 14(1): 4031, (2023).

[13] Dege, N., Gökçe, H., Doğan, O. E., Alpaslan, G., Ağar, T., Muthu, S. Sert, Y., "Quantum computational, spectroscopic investigations on N-(2-((2-chloro-4,5-dicyanophenyl)amino) ethyl)-4-methylbenzenesulfonamide by DFT/TD-DFT with different solvents, molecular docking and drug-likeness researches", Colloid Surface A, 638: 128311, (2022).

[14] Bilkan, M. T., Alyar, S., Alyar, H., "Experimental Spectroscopic and Theoretical Studies of New Synthesized Sulfonamide Derivatives", Russian Journal of Physical Chemistry A, 94: 143-151, (2020).

[15] Alyar, S., Bilkan, M. T., Karataş, M. F., Bilkan, Ç., Alyar, H., "Experimental and Theoretical Studies on A New Sulfonamide Derivative and Its Copper Complex: Synthesis, FT-IR, NMR, DFT, Molecular Docking and In Silico Investigations", Journal of Molecular Structure, 137531, (2024).

[16] Dennington, R. D., Keith, T. A., Millam, J. M., GaussView 5, Gaussian, Inc., (2008).

[17] Frisch, M. J., et al., Gaussian 09, Revision B.01, Gaussian Inc., C.T. Wallingford, (2009).

[18] Jamróz, M. H., Vibrational Energy Distribution Analysis. VEDA 4, Warsaw, (2004).

[19] Parr, R. G., Szentpa´ly, L.V., Liu, S., "Computational Analysis of Theacrine, a Purported Nootropic and Energy-Enhancing Nutritional Supplement", Journal of the American Chemical Society, 121: 1922-1924, (1999).

[20] Bitencourt-Ferreira, G., and de Azevedo, W. F., "Molegro virtual docker for docking", Docking Screens for Drug Discovery, 149-167, (2019).

[21] PreADMET, https://preadmet.qsarhub.com/, (2022).

[22] ProTox-II- Prediction of Toxicity of Chemicals, (2022).

[23] Ji, Y., Yang, X., Ji, Z., Zhu, L., Ma, N., Chen, D., Jia, X., Tang, J., and Cao, Y., "DFT-calculated IR spectrum amide I, II, and III band contributions of N-methylacetamide fine components", ACS Omega, 5(15): 8572-8578, (2020).

[24] Franke, P. R., Stanton, J. F., and Douberly, G. E., "How to VPT2: Accurate and intuitive simulations of CH stretching infrared spectra using VPT2+ K with large effective Hamiltonian resonance treatments", The Journal of Physical Chemistry A, 125(6): 1301-1324, (2021).

[25] Anderson, R. J., Bendell, D. J., Groundwater, P. W., "Organic spectroscopic analysis", Royal Society of Chemistry, (2004).

[26] Gunawan, R., Nandiyanto, A. B. D., "How to read and interpret 1H-NMR and 13C-NMR spectrums", Indonesian Journal of Science and Technology, 6(2): 267-298, (2021).

[27] Bilkan, M. T., Yurdakul, Ş., Demircioğlu, Z., Büyükgüngör, O., "Crystal structure, FT-IR, FT-Raman and DFT studies on a novel compound $[C_{10}H_9N_3]_4.AgNO_3$", Journal of Organometallic Chemistry, 805: 108-116, (2016).

[28] Bilkan, M. T., "Quantum chemical studies on solvent effects, ligand–water complexes and dimer structure of 2,2′-dipyridylamine", Physics and Chemistry of Liquids, 57: 100-116, (2019).

[29] Lee, M. S., Kerns, E. H., "LC/MS applications in drug development", Mass Spectrometry Reviews, 18(3-4): 187-279, (1999).

[30] Supuran, C. T., "Carbonic anhydrases-an overview", Current Pharmaceutical Design, 14(7): 603-614, (2008).

[31] Supuran, C. T., Scozzafava, A., "Carbonic anhydrases as targets for medicinal chemistry", Bioorganic & Medicinal Chemistry, 1: 4336-50, (2007).

[32] Supuran, C. T., "Carbonic anhydrases--an overview", Current Pharmaceutical Design, 14: 603-614, (2008).

[33] Butina, D., Segall, M. D., Frankcombe, K., "Predicting ADME properties in silico: methods and models", Drug Discovery Today, 7: 83-88, (2002).

[34] Ma, X. L., Chen, C., Yang, J., "Predictive model of blood-brain barrier penetration of organic compounds", Acta Pharmacologica Sinica, 26: 500-512, (2005).

[35] Lea, T., Caco-2 Cell Line, "The Impact of Food Bioactives on Health in Vitro and Ex Vivo Models", Springer, Cham, Chapter 10, (2015).

[36] Yamashita, S., Furubayashi, T., Kataoka, M., Sakane, T., Sezaki, H., Tokuda, H., "Optimized conditions for prediction of intestinal drug permeability using Caco-2 cells", European Journal of Pharmaceutical Sciences, 10(3): 195-204, (2000).

[37] Christopher, A. L., “Lead- and drug-like compounds: the rule-of-five revolution”, Drug Discovery Today Technologies, 1: 337-341, (2004).

[38] "Absolute lethal dose (LD100)", IUPAC Gold Book. International Union of Pure and Applied Chemistry, Archived from the original on 2019-07-01, Retrieved, (2019).

[39] "What is a LD50 and LC50?", OSH Answers Fact Sheets. Canadian Centre for Occupational Health and Safety, 5 October, (2021).

[40] Copper Toxicity, “Fundamentals of Toxicologic Pathology (Second Edition)”, (2010).

[41] Janssen, J., Saluja, S. S., “How much did you take? Reviewing acetaminophen toxicity”, Canadian Family Physician, 61: 347-356, (2015).